University of
Strathclyde
Glasgow

Strathprints Institutional Repository

Maddock, Christie and Vasile, Massimiliano (2008) *Extension of the proximity-quotient control law for low-thrust propulsion.* In: 59th International Astronautical Congress, 2008-09-29 - 2008-10-03, Glasgow, Scotland.

http://strathprints.strath.ac.uk/

IAC-08-C1.5

EXTENSION OF THE PROXIMITY-QUOTIENT CONTROL LAW FOR LOW-THRUST PROPULSION

CHRISTIE ALISA MADDOCK

Space Advanced Research Team, Department of Aerospace Engineering,
University of Glasgow, United Kingdom G12 8QQ
email: c.maddock@aero.gla.ac.uk

MASSIMILIANO VASILE

Space Advanced Research Team, Department of Aerospace Engineering,
University of Glasgow, United Kingdom G12 8QQ
email: mvasile@aero.gla.ac.uk

ABSTRACT

In this paper, the proximity quotient control law, first developed by Petropoulos, is extended to account for both third body effects and solar radiation pressure. The perturbing effect of solar radiation pressure becomes relevant when dealing with solar sails, or large optics in space. Equations for the disturbing acceleration and disturbing potential function were derived for the perturbations, then analyzed to determine the minimum and maximum rate of changes of the Keplerian elements given the thrust vector and true anomaly of the spacecraft. These were then analytically incorporated into the Q-law feedback function. The complete mathematical derivations are presented. The extended Q-law is compared to the fully optimal control law, stemming from optimal control theory, for the same dynamical model. Two missions are used as test cases.

1 INTRODUCTION

The proximity-quotient control law, or Q-law, was first proposed by Petropoulos (2003) to generate first guess approximations for propellant-optimal, low-thrust transfers between two Keplerian orbits. It is based on a Lyapunov feedback control law and calculates the optimal direction of thrust based on the proximity to the target orbit (i.e. the difference in the static Keplerian parameters) and the current location of the spacecraft on the orbit (i.e. true anomaly). The basic Q-law was developed for the restricted two-body problem, based on Gauss' planetary equations.

In this paper, this Q-law is extended to account for both third body effects and solar radiation pressure. The perturbing effect of solar radiation pressure becomes relevant when dealing with solar sails, or large optics in space. Equations for the disturbing acceleration and disturbing potential function were derived for the perturbations, then analyzed to determine the minimum and maximum rate of changes of the Keplerian elements given the thrust vector and true anomaly of the spacecraft. These were then analytically incorporated into the Q-law feedback function. The complete mathematical derivations are presented.

By accounting for the additional perturbations within the control law, this allows for a better optimization of the resulting transfer. The resulting Q-law is compared to the fully optimal control law, stemming from optimal control theory, for the same dynamical model. Two mis-

sions are used as test cases. The first calculates the transfer trajectories following the initial deployment of a formation of spacecraft, into their final formation orbits. The second covers a more complex test case based on an asteroid deviation mission, where each spacecraft in the formation is required to constantly adjust their orbits in order to maintain a periodic motion with respect to the asteroid.

…

In general, NEO deflection techniques fall into four broad categories [7]: kinetic impacts, propulsive devices, induced changes to the asteroid surface, and ablation devices. A previous study by the authors compared the various deflection methods in terms of: achieved deviation distance, required warning time, total mass into orbit and the estimated technology readiness level. The solar sublimation technique was found to be among the most effective methods. The idea was initially proposed [2] in 1992 and was compared a year later to other deflection methods by Melosh [5]. The concept envisions a large mirror in space which would reflect sunlight onto the surface of the asteroid, sublimating the material and generating a low, continuous thrust due to the force of the ejected debris.

Further preliminary studies were undertaken determining the feasibility of such a mission, and developing an initial design for the mirror assembly and orbit of…

2 DESCRIPTION OF THE TEST CASES

The following section describes the assumptions and design used for NEO deflection mission using a solar sublimation technique, here used as the test case.

2.1 Spacecraft Mirror Assembly Design

Fig. 1 shows the mirror configuration design on-board the spacecraft. The primary mirror is paraboloidic in shape, and focuses the rays onto a collimating lens (or system of lenses). The collimated beam is then directed by a smaller flat mirror onto the desired location on the asteroid surface. Due to the large required surface area of the primary mirror, e.g. diameter between 10-30m, any control law must accommodate the perturbations caused by the solar radiation pressure (SRP).

The illuminated surface area is calculated based on the focal length l_f,

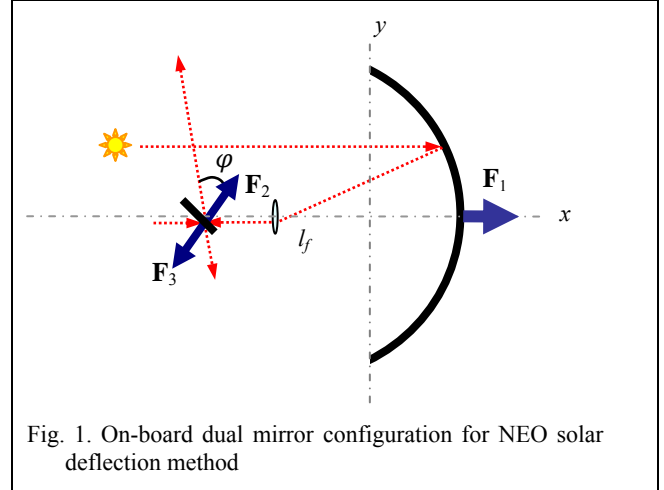$$l_f = \frac{d_p}{4\sqrt{l_{offset}}} \qquad (1)$$

Fig. 1. On-board dual mirror configuration for NEO solar deflection method

and accounting for the blockage caused by the secondary mirror,

$$A_p = \iint_{y\,x} 4\sqrt{\left(\frac{x}{2l_f}\right)^2 + \left(\frac{y}{2l_f}\right)^2 + 1}\; dx\,dy \qquad (2)$$

where d_p is the diameter of the aperture on the parabolic mirror, d_d is the diameter of the directional flat mirror and φ is the angle of reflection. The depth of the mirror is given in terms of a percent of the focal length, l_{offset} set here to 80%. Clearly, the optimal depth would be equal to the focal length, however practically it is governed by the maximum allowable angle of incidence of the lens. It is also necessary to ensure that the flat mirror does not reflect the beam back onto any part of the parabolic mirror due to both blockage, and temperature concerns.

The integrals in (2) are bounded by a lower limit of $(d_d/2)\cos\varphi$, and an upper bound of $d_p/2$.

2.2 Formation Orbit Design

The spacecraft have to maintain their relative position with respect to the asteroid in order to keep the required power density on the same spot of the surface of the asteroid. Therefore, the formation orbits have to be periodic and in close proximity with low excursion in the relative distance from the asteroid. On the other hand the spacecraft should avoid, as much as possible, to fly in the irregular regions of the gravity field of the asteroid. In addition, should also avoid any impingement with the plume of debris and gas coming from the sublimation of the surface material.

In order to design the desired formation orbits, we start by considering the linearised relative equations of motion [8],

$$x = \frac{r}{a}\delta a - a\cos f\, \delta e + \frac{ae\sin f}{\eta}\delta M \qquad (3)$$

$$y = \frac{r\sin f}{\eta^2}\left(2 + e\cos f\right)\delta e + r\cos i\,\delta\Omega + r\delta\omega$$
$$+ \frac{r}{\eta^3}\left(1 + e\cos f\right)^2 \delta M \qquad (4)$$

$$z = r\sin\theta\,\delta i - r\cos\theta\sin i\,\delta\Omega \qquad (5)$$

$$\dot{x} = \frac{\dot{r}}{a}\delta a + a\dot{f}\sin f\,\delta e + \frac{ae\dot{f}\cos f}{\eta}\delta M \qquad (6)$$

$$\dot{y} = \left(\left(2 + e\cos f\right)\left(\dot{r}\sin f + r\dot{f}\cos f\right) - re\dot{f}\sin^2 f\right)\frac{\delta e}{\eta^2}$$
$$+ \dot{r}\cos i\,\delta\Omega + \dot{r}\delta\omega \qquad (7)$$
$$+ \left(1 + e\cos f\right)\left(\dot{r}\left(1 + e\cos f\right) - 2re\dot{f}\sin f\right)\frac{\delta M}{\eta^3}$$

$$\dot{z} = \left(\dot{r}\sin\theta + r\dot{f}\cos\theta\right)\delta i - \sin i\left(\cos\theta - r\dot{f}\sin\theta\right)\delta\Omega \qquad (8)$$

where

$$\dot{r} = re\dot{f}\sin f \quad \dot{f} = \frac{h}{r^2} \quad \eta = \sqrt{1 - e^2}$$

which use the orbital element differences between a chief orbit (which can be virtual, and is located at the origin of the Hill reference frame) and a spacecraft in the formation [8]. This is a first approximation of the motion of the spacecraft that does not take into account the gravity field of the asteroid and the solar pressure but it is useful to identify some orbit geometries that answer to our requirements.

The orbital dynamics for the formation are relative to two rotating Hill reference frames, one centered on the asteroid $\mathcal{A}$, and the other centered on the spacecraft $\mathcal{S}$, both in the local radial x, transversal y and normal z directions (see Fig. 2).

The formation orbit can be thought of as an orbit around the Sun with a small offset in the initial position $\delta\mathbf{r}_0$ and velocity $\delta\mathbf{v}_0$. This offset can also be expressed as the difference between the orbital parameters of the chief (e.g. Apophis) and the formation. As long as there is no difference in semi-major axes, the two orbits will remain periodic.

$$\delta\mathbf{k} = \mathbf{k}_s - \mathbf{k}_A = \begin{bmatrix} \delta a & \delta e & \delta i & \delta\Omega & \delta\omega & \delta M \end{bmatrix} \qquad (9)$$
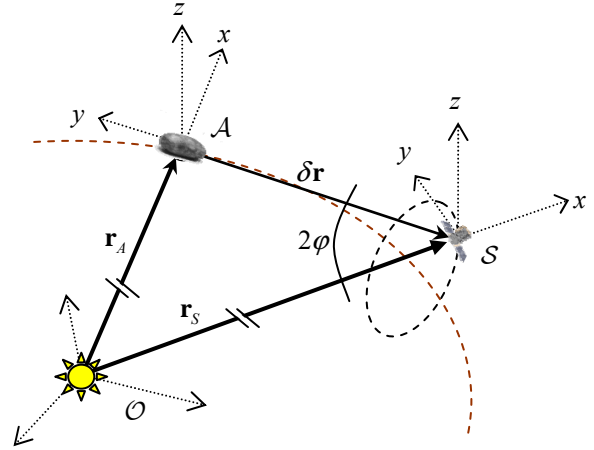

Fig. 2. Relative reference frames used in the orbital determination for the formation.

As the mean anomaly is a function of the semi-major axis, the difference in mean anomaly will remain constant throughout the orbit so long as $\delta a = 0$.

If the optimal thrust direction that maximizes the deviation is along the unperturbed velocity vector of the asteroid [10], then the exhaust gases will flow along the y-axis of the local Hill reference frame. Therefore, the size of the formation orbits projected in the x-z plane should be maximal. All the requirements on the formation orbits can be formulated in mathematical terms as a multi-objective optimization problem,

$$\min_{\delta\mathbf{k}\in D}\min_f J_1 = \delta\mathbf{r} \qquad (10)$$

$$\min_{\delta\mathbf{k}\in D}\min_f J_2 = -\sqrt{x^2 + z^2} \qquad (11)$$

subject to the constraint

$$C_{ineq} = \min_f\left(\delta r(f) - r_{lim}\right) > 0 \qquad (12)$$

where r_{lim} is a minimum-radius sphere imposed to avoid non-linearities in the asteroid gravity field [7], and D is the search space for the solution vector $\delta\mathbf{k}$.
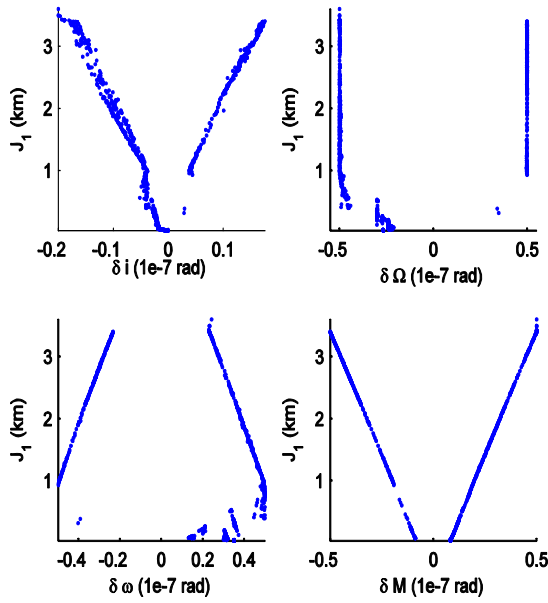
Fig. 3. δ**k** parameters for the set of Pareto optimal solutions versus objective function J_1
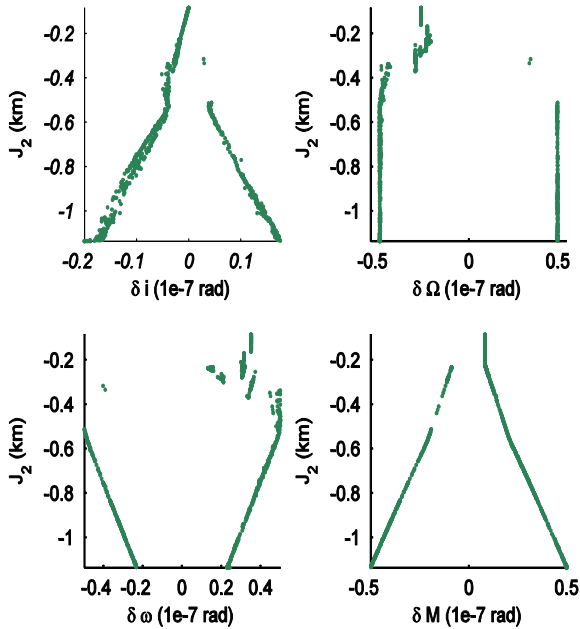

Fig. 4. δ**k** parameters for the set of Pareto optimal solutions versus objective function J_2

The objective functions in (10)-(11) were solved with a hybrid stochastic-deterministic approach based on a multi-agent search technique combined with a decomposition of the search space [4][11]. The result was several groupings of formation orbits. As can be seen in **Error! Reference source not found.** and Fig. 4 the solutions are symmetrically distributed about the axis where the δ**k**

parameters are zero. The existence of families can be seen, for example, through δΩ and δω, where for a given input value there are multiple values for the objective functions J_1 and J_2. Fig. 5 shows the formation orbits in the 𝒜 Hill frame. These solutions belong to four symmetric families of formation orbits, each one corresponding to a funnel.
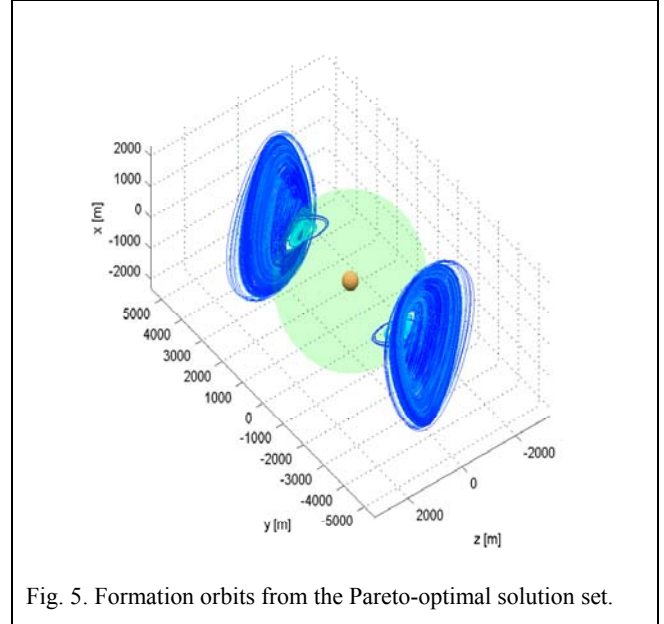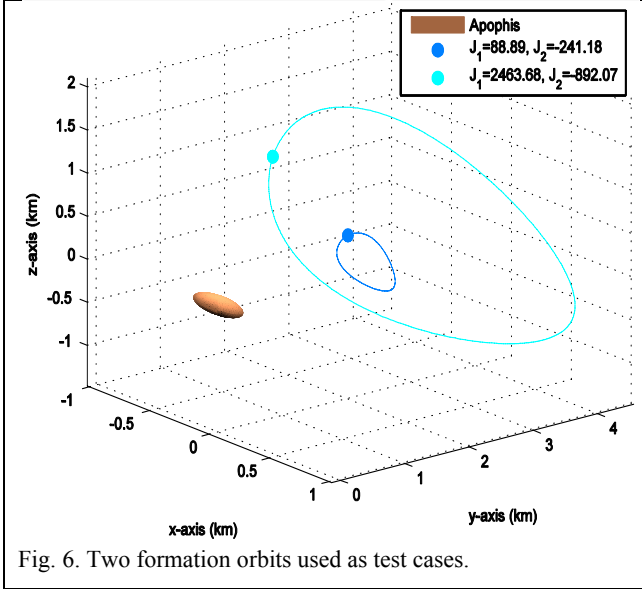

Fig. 5. Formation orbits from the Pareto-optimal solution set.

Table 1. Optimized initial conditions for formation orbit test cases at t_0 = 11429.75 MJD2000.

Parameter	Value	
J_1 (m)	88.8845	2463.6755
J_2 (m)	-241.1802	-892.0682
δa (km)	0	0
δe	6.9071E-12	-5.7472E-13
δi (rad)	-1.7903E-09	-1.2645E-08
δΩ (rad)	-2.3827E-08	-5.0000E-08
δω (rad)	3.1574E-08	3.3794E-08
δM (rad)	8.9855E-09	3.7997E-08

Two representative formation orbits were chosen out of the Pareto-optimal set to test the control laws. The values for the initial δ**k** are given in Table 1. The initial time was set to 5 years prior to the estimated date of impact on 13 April 2036. Note, this is the start of the thrusting maneuver, not the launch date from Earth.

Fig. 6. Two formation orbits used as test cases.

$$\mathbf{u} = \begin{bmatrix} u_x \\ u_y \\ u_z \end{bmatrix} = \begin{bmatrix} u\sin\alpha\cos\beta \\ u\cos\alpha\cos\beta \\ u\sin\beta \end{bmatrix} \quad (18)$$

in the radial x, transversal y and normal z directions, $\mathbf{k} = [a, e, i, \Omega, \omega, f]$ is the set of Keplerian orbit elements, $\theta = f + \omega$ is the true latitude, $p = a(1-e^2)$ is the semi-latus rectum, μ is the gravitation constant of the central body, n is the mean motion and h is the angular momentum.

Analytical equations were found for the direction of thrust $[\alpha, \beta]$ and true anomaly f that maximized the rate of change of each orbital element, $\dot{k}_{xx}$. Since the Q-law was designed for transfer trajectories between two Keplerian orbits (and not "point-to-point" transfers), the rate of change of the true (or mean) anomaly was ignored.
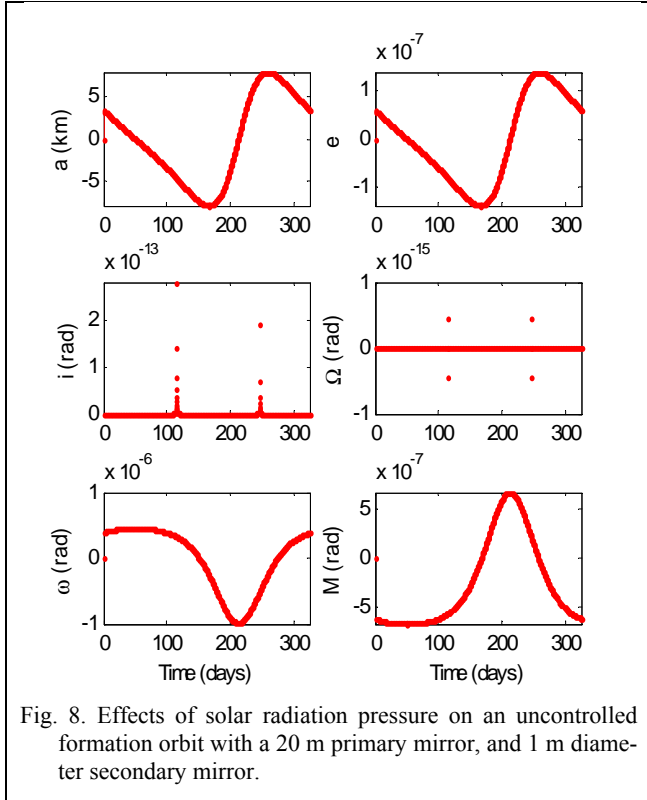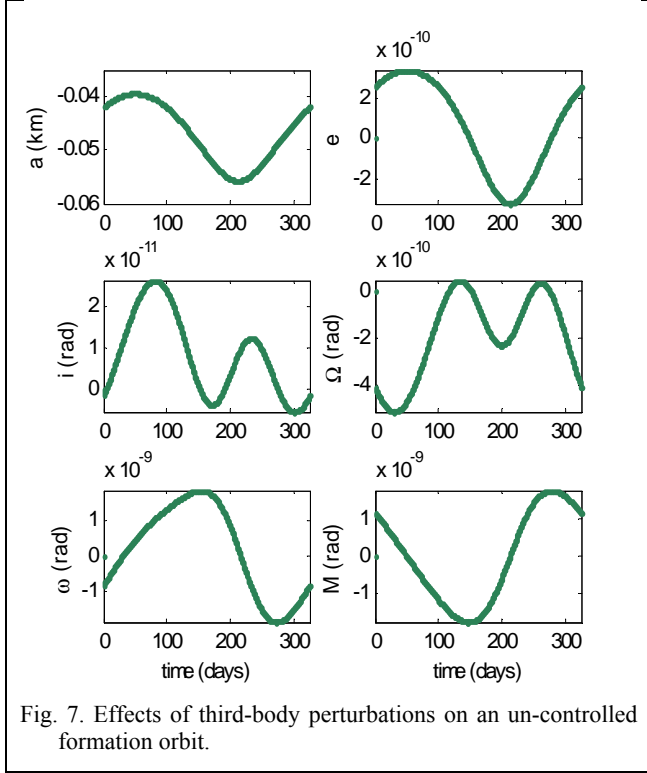
These maximized rates of change were summed, along with the desired difference in the time-invariant Keplerian parameters to generate the *proximity-quotient* equation [6].

$$Q = \sum_{\mathbf{k}}^{5} W_k \left(\frac{k_i - k_T}{\dot{k}(\alpha_{max}, \beta_{max}, f_{max})} \right)^2 \rightarrow \min_{\alpha,\beta} \dot{Q}(\mathbf{k}_i, \mathbf{k}_T) \quad (19)$$

where W_k are a set of weights between [0 1], i and T are the initial and target states, and $\mathbf{k} = [a \ e \ i \ \Omega \ \omega \ f]$. The Lyapunov function is simply the rate of change of Q with time. The partial derivates of Q for each of the first five elements in $\mathbf{k}$ can be solved analytically. The optimal thrust angles at any point in time can be determined by finding the global minimum of dQ/dt.

3   CONTROL LAW EXTENSIONS

3.1   *Q*-law Control

The proximity-quotient control law, or *Q*-law, was first proposed by Petropoulos [6] in 2003 to generate first guess approximations for propellant-optimal, low-thrust transfers between two Keplerian orbits. It is based on a Lyapunov feedback control law and calculates the optimal direction of thrust $[\alpha, \beta]$ based on the proximity to the target orbit (i.e. the difference in the static Keplerian parameters) and the current location of the spacecraft on the orbit (i.e. true anomaly f). The basic *Q*-law was developed for the restricted two-body problem, based on Gauss' planetary equations, given below [1].

$$\frac{da}{dt} = \frac{2a^2}{h}\left((e\sin f)u_x + \frac{p}{r}u_y \right) \quad (13)$$

$$\frac{de}{dt} = \frac{(p\sin f)u_r + ((p+r)\cos f + re)u_t}{h} \quad (14)$$

$$\frac{di}{dt} = \frac{r\cos\theta}{h}u_h \quad (15)$$

$$\frac{d\Omega}{dt} = \frac{r\sin\theta}{h\sin i}u_h \quad (16)$$

$$\frac{d\omega}{dt} = \frac{(-p\cos f)u_r + ((p+r)\sin f)u_t}{he} \quad (17)$$
$$\qquad\qquad - \frac{r\sin\theta\cos i}{h\sin i}u_t$$

where $\mathbf{u}$ represents the disturbing acceleration,

3.2   Technical Limitations

For the maintenance of the formation orbit, a number of issues that arose when using the *Q*-law: the first was due to the high degree of accuracy need to maintain the funnel orbits. The difference in Keplerian between the NEO and the spacecraft are on the order of 10^{-7}, and need to remain constant even as the NEO deviates. This resulted in a lot of 'chatter' (over-shooting) around the target orbital elements, due to strong dependence on the time step δt and the magnitude of the control (which employed on-off shooting). Even at very small time steps, the magnitude of the over-shooting was too large for the system requirements. In addition, the effects of the individual perturbations are relatively large (shown in **Error! Reference source not found.** and **Error! Reference source not found.**) and need to be compensated for on a continuous basis.

Fig. 7. Effects of third-body perturbations on an un-controlled formation orbit.

Fig. 8. Effects of solar radiation pressure on an uncontrolled formation orbit with a 20 m primary mirror, and 1 m diameter secondary mirror.

Therefore a variant of the *Q*-law was developed to account for these limitations. Specifically: the inclusion of SRP and gravitational effects of the asteroid in the

determined rate of change of the orbital elements, and inclusion of compensation for the disturbances to the mean anomaly δ*M*.

3.3 Perturbations

The general equation for the magnitude of acceleration due to solar radiation pressure is,

$$\ddot{\mathbf{r}}_{SRP} = \frac{2S_0}{c} \frac{\eta_{eff} A}{m_s} \left(\frac{r_{1AU}}{r_s} \right)^2 \cos^2 \varphi \cdot \hat{\mathbf{n}} \qquad (20)$$

where S_0 is the solar flux density at 1 AU (1367 W/m^2), c is the speed of light, η_{eff} is the efficiency, A is the surface area, m_s is the mass of the spacecraft, r_s is the distance between the Sun and the spacecraft, and lastly φ is the angle of reflection. The SRP always acts in the direction normal $\hat{\mathbf{n}}$ to the mirror surface.

As the primary mirror is always aligned with the Sun, the net force $\mathbf{F}_1$ is inline with the radial direction in the spacecraft-centric reference frame $\mathcal{S}$. For the secondary mirror, two forces are accounted for: $\mathbf{F}_2$, the reflected SRP from the primary mirror, and $\mathbf{F}_3$, the force due to the SRP from the Sun acting on the 'back' of the mirror (see Fig. 1).

$$\mathbf{F}_1 \Rightarrow \mathbf{s}_p = \frac{2P_0}{mr_s^2} \eta A_p \cdot \hat{\mathbf{x}} \qquad (21)$$

$$\mathbf{F}_2 + \mathbf{F}_3 \Rightarrow \mathbf{s}_d = \frac{2P_0}{mr_s^2} \eta \cos^2 \varphi \left(A_d - \eta A_p \right) \cdot \frac{\mathbf{n}_d}{\|\mathbf{n}_d\|} \quad (22)$$

where $P_0 = r_{1AU}^2 S_0/c$. In the following we will take into account only the contribution of the forces due to the orbital dynamics but it should be noted that the combination of $\mathbf{F}_2$ and $\mathbf{F}_3$ will induce a consistent torque on the mirror assembly.

The unit vector for the direction of the solar pressure on the direction mirror $\hat{\mathbf{n}}_d$ is derived in terms of Keplerian orbital elements relative to the Hill frame centered on the spacecraft.

$$\mathbf{n}_d = \begin{bmatrix} -\sqrt{\dfrac{\varpi}{2\delta r}}\left(r_S + r_A\zeta_2\cos\theta + r_A\zeta_3\sin\theta\right) \\[2ex] r_A\left(\cos i\cos(\delta\theta-\theta)\cos\theta\sin\delta\Omega \\ +\zeta_1\cos\theta\sin(\delta\theta-\theta)-\zeta_2\sin\theta\right) \\[2ex] r_A\left(\cos(\delta\theta-\theta)\sin\delta\Omega\sin i + \xi\sin(\delta\theta-\theta)\right) \\ \cdot\left(\sqrt{\dfrac{2\varpi}{\delta r}}+r_S\left(r_S + r_A\zeta_2\cos\theta + r_A\zeta_3\sin\theta\right)\right) \end{bmatrix} \quad (23)$$

where

$$\zeta_1 = \cos i\sin(\delta i - i) + \cos\delta\Omega\cos(\delta i - i)\sin i \quad (24)$$

$$\zeta_2 = \cos\delta\Omega\cos(\delta i - i)\cos i - \sin(\delta i - i)\sin i \quad (25)$$

$$\zeta_3 = -\cos\delta\Omega\cos(\delta\theta-\theta) \\ + \cos(\delta i - i)\sin\delta\Omega\sin(\delta\theta-\theta) \quad (26)$$

$$\xi = \cos i\cos(\delta\theta-\theta)\sin\delta\Omega + \zeta_1\sin(\delta\theta-\theta) \quad (27)$$

$$\varpi = \delta r + r_S - r_A\big(\cos\delta\Omega\cos(\delta\theta-\theta)\cos\theta \\ + \cos(\delta i - i)\cos\theta\sin\delta\Omega\sin(\delta\theta-\theta)+\zeta_3\sin\theta\big) \quad (28)$$

Similarly, the vector from the spacecraft to the asteroid, $\delta\mathbf{r}$, can be expressed in the spacecraft-centered Hill reference frame $\mathcal{S}$ by means of geometry.

$$\delta\mathbf{r}^S = \mathbf{r}_S - \mathbf{r}_A \\ = \begin{bmatrix} -r_S - r_A\left(\zeta_2\cos\theta + \zeta_3\sin\theta\right) \\ -r_A\left(-\zeta_3\cos\theta + \zeta_2\sin\theta\right) \\ -r_A\left(-\cos(\delta\theta-\theta)\sin\delta\Omega\sin i - \xi\sin(\delta\theta-\theta)\right) \end{bmatrix} \quad (29)$$

Note that it is also possible to use the linearised equations of motion in (3)-(8) as long as $\delta r \ll r_s$, however since the computation time is the same, the more exact equations were used.

Lastly, the angle of reflection is re-derived in terms of the orbital elements,

$$\cos^2\varphi = \frac{r_A{}^2\left(\cos(\delta\theta-\theta)\sin\delta\Omega\sin i + \xi\sin(\delta\theta-\theta)\right)^2}{\left|2\varpi\delta r\right|} \quad (30)$$

Since the effects of the asteroid's gravity field outside the imposed limiting sphere are relatively linear [7], and much less compared to those due the solar radiation pressure, the asteroid is treated, as a first approximation, as a point mass with $\mu_A = 1.8016\text{E-}9$ km^3/s^2 (the mass is taken as 2.7E9 kg).

The Gauss equations in (13) can be re-expressed using a modified disturbing acceleration vector accounting for the solar radiation pressure, and the third body effects.

$$\mathbf{u}_{pert} = \begin{bmatrix} s_p + (s_d)_x - \dfrac{\mu_A}{\delta r^3}x \\[2ex] (s_d)_y - \dfrac{\mu_A}{\delta r^3}y \\[2ex] (s_d)_z - \dfrac{\mu_A}{\delta r^3}z \end{bmatrix} \quad (31)$$

3.4 Mean anomaly

Due to the nature of the formation orbits, the difference in mean anomaly must also be controlled. As such, the rate of change due to the perturbations for M was added to the modified Gauss equations. In this case, the rotation around the Sun ($n\delta t$) is not considered as an unwanted perturbation, and is accounted outside the control law.

$$\frac{dM^*}{dt} = \frac{(p\cos f - 2re)u_x - ((p+r)\sin f)u_y}{e\sqrt{a\mu}} \quad (32)$$

3.5 Integration Approach

In addition to accounting for the above perturbations within the control law, a number of changes were introduced to further refine the algorithm to the specific test case. The first was to switch from minimizing only the thrust angles $[\alpha,\beta]$, to directly minimizing the components $[u_x, u_y, u_z]$ which has the benefit of finding the optimal magnitude for the thrust, as well as the required angles. The new control function is given by,

$$Q^* = \sum_{j=1}^{6}\left(\Delta k_{T,j} - \int_0^{\delta t}\frac{dk_j}{dt}dt\right)^2 \quad (33)$$

where $\Delta\mathbf{k}_T = \left(\mathbf{k}_i - \mathbf{k}_T\right)$ is the desired variation of the orbital parameters over the time interval δt.

The function Q^* is then minimized with respect to the applied control $\mathbf{u}_c$. Inherently, if the desired change in the jth element $(k_{i,j} - k_{T,j})$ is negative, than the rate of change is positive, and vice versa. As such, the control equation will always have a single minimum. Therefore there is no need to minimize the time derivative.

3.6 Least Squares Approach

If we consider that over very small time steps, we can assume as first approximation that the orbital parameters

in the Gauss equations are constant, than we can solve directly for control function Q^*. The solution for the control vector **u** is found by using an ordinary least squares fitting to the linear systems of equations $\mathbf{Au}_c = \mathbf{b}$. Here, the matrix **A** is set equal to the Gauss equations as a function of the applied control $\mathbf{u}_c$ only (i.e. no perturbations). The second vector **b** is given by,

$$\mathbf{b} = \frac{\mathbf{k}_i - \mathbf{k}_T}{\delta t} - \mathbf{A}(\mathbf{u}_{pert}) \qquad (34)$$

where $\mathbf{u}_{pert}$ is given in (31).

Again, this is equivalent to minimizing the quadratic function $\Sigma\left(\Delta\mathbf{k}_{i,j} - \Delta\mathbf{k}_{T,j}\right)^2$ where $\Delta\mathbf{k}_{i,j}$ is the change of the jth orbital element over time δt calculated using the Gauss equations, and $\Delta\mathbf{k}_{i,T}$ is the desired change. Weights can also be used to scale individual $\delta\mathbf{k}$ parameters to increase (or decrease) their sensitivity.

3.7 Integration Approach

The least-squares approach provides a computationally faster (for the same time step) but less accurate, especially over larger time steps. The integration approach uses the same control function Q^* however numerically integrates the Gauss equations to determine $\Delta\mathbf{k}_{i,j}$.

4 SIMULATION RESULTS

The algorithm used to simulate the deflection mission is given below.

STEP 1: Initialize starting conditions at t_0 for each spacecraft and NEO, $\mathbf{k}_T = \mathbf{k}_i = \mathbf{k}_0$.

STEP 2: Determine optimal control vector $\mathbf{u}_c$ solving using either the least-squared method or integration method, given current state $\mathbf{k}_i$, target state $\mathbf{k}_T$, and position of the deviated asteroid $\mathbf{k}_A$.

STEP 3: Propagate **r**, **v** forward by time step δt using Gauss equations with input ($\mathbf{u}_c + \mathbf{u}_{pert}$), and update the current state $\mathbf{k}_i(t + \delta t)$.

STEP 4: Propagate asteroid given thrust due to the solar sublimation again by numerically integrating Gauss equations, and update $\mathbf{k}_A(t + \delta t)$. Note: a description for the method for determining the generated thrust can be found in [7].

STEP 5: Update target state, $\mathbf{k}_T(t + \delta t) = \mathbf{k}_A + \delta\mathbf{k}$.

REPEAT from STEP 2 until achieved deviation is achieved.

5 CONCLUSION

ACKNOWLEDGMENTS

REFERENCES

[1] Battin R. H., *An Introduction to the Mathematics and Methods of Astrodynamics*, Rev. ed., AIAA Education Series, Virginia USA, 1999.

[2] Lunan, D., "Need we protect Earth from space objects and if so, how?", *Space Policy*, Vol. 8, No. 1, 1992, pp. 90-91.

[3] Maddock C., Sanchez Cuartielles J. P., Vasile M., Radice G., "Comparison of Single and Multi-spacecraft Configurations for NEA Deflection by Solar Sublimation", *Proceedings from New Trends in Astrodynamics and Applications III*, AIP, Vol. 886, Issue 1, 2007, pp. 303-316.

[4] Maddock C., Vasile M., "Design of optimal spacecraft-asteroid formations through a hybrid global optimisation approach", *International Journal of Intelligent Computing and Cybernetics*, Vol. 1, No. 2, 2008, pp. 239–268.

[5] Melosh H. J., Nemchinov I. V. and Zetzer Y. I., "*Hazard due to Comets and Asteroids*", University of Arizona Press, 1994, pp. 1111-1132.

[6] Petropoulous A., "Simple Control Laws for Low-Thrust Orbit Transfers", *AIAA/AAS Astrodynamics Specialists Conference*, Montana USA, August 2003.

[7] Sanchez Cuartielles J. P., Colombo C., Vasile M., Radice G., "Multi-criteria Comparison among Several Mitigation Strategies for Dangerous Near Earth Objects", *Journal of Guidance and Control*, [to be published], Accepted 2008.

[8] Schaub H., Junkins J. L., *Analytical Mechanics of Space Systems*, AIAA Education Series, Virginia, 2003.

[9] Vasile M., "A Multi-Mirror Solution for the Deflection of Dangerous NEOs", *Conference on Nonlinear Science and Complexity*, July 2008.

[10] Vasile M., Colombo C., "Optimal Impact Strategies for Asteroid Deflection", *Journal of Guidance, Control and Dynamics*, Vol. 31, No. 4, 2008, pp. 858–872.

[11] Vasile M., *Multi-Objective Memetic Algorithms*, Hybrid Behavioral-Based Multiobjective Space Trajectory Optimization, Studies in Computational Intelligence, Springer, 2008.